Triarylpyridinium-Functionalized Terpyridyl Ligand for Photosensitized Supramolecular Architectures: Intercomponent Coupling and Photoinduced Processes**

Philippe Lainé,*[a] Fethi Bedioui,[b] Edmond Amouyal,[a] Valérie Albin,[b] and Florence Berruyer-Penaud[a]

Abstract: The electronic (absorption spectra) and electrochemical properties of a novel series of triphenylpyridinium ($H_3TP^+ = A$) electron-acceptor-based polyad species have been correlated with their steady-state (emission spectra) and time-resolved (ns and ps laser flash photolysis) photophysical behavior (at both 293 and 77 K). These d^6 transition metal complexes ($M = Ru^{II}$, Os^{II}) of 2,2′:6′,2″-terpyridines (tpy) are denoted as P0 and P1, depending on whether they incorporate H_3TP^+-tpy or H_3TP^+-ptpy ligands (ptpy = 4′-phenyl-substituted tpy), respectively. For the P0/Ru-based compounds, the luminescence quantum yield and excited-state lifetime of the "$\{Ru(tpy)_2\}^{2+}$" chromophore have been found to be considerably enhanced at 293 K (e.g., $\tau = 0.56$ ns for isolated P0/Ru in acetonitrile vs $\tau = 55$ and 27 ns for P0/Ru within P0A/Ru and P0A_2/Ru (A = electron acceptor), respectively). In spite of the lack of conjugation between P0 and A, this behavior has been ascribed to a through-bond mediated electronic substituent effect originating from the directly connected H_3TP^+ electron-withdrawing group. For the P1-based compounds, the possibility of photoinduced electron-transfer (PET) processes with the formation of charge-separated (CS) states is discussed, and the main results may be summarized as follows: 1) when involved, the electron-donor D (D = Me_2N of Me_2N-ptpy) is strongly electronically coupled to P1 but cannot facilitate a reductive quenching of *P1 to give the *[$D^+ - P1^-$]-type of CS state for thermodynamic reasons, irrespective of whether M is Ru^{II} or Os^{II}; 2) the P1 and A components have been shown to be very weakly electronically coupled; 3) at 293 K, P1/Ru- and P1/Os-based polyad systems display distinct photophysical behavior with respect to A, with only the latter exhibiting a noticeable quenching of luminescence (up to 50% for P1A/Os with respect to P1/Os); 4) for assemblies made up of P1/Os and A components only, comparison between their room-temperature (RT) and low-temperature (LT; 77 K, frozen matrix) photophysical properties, together with information gleaned from combined transient absorption experiments and spectroelectrochemical studies of P1/Os and P1A/Os, further supported by thermodynamic considerations, allowed us to conclude that a PET process does take place within the P1A/Os dyad leading to the *[$P1^+ - A^-$] CS state. For the DP1A/Os triad, the formation of such a CS state followed by an enhanced electron-releasing inductive effect from D is postulated.

Keywords: donor–acceptor systems · electrochemistry · electron transfer · luminescence · supramolecular chemistry

Introduction

The field of supramolecular chemistry[1] provides a conceptual framework for research devoted to the mimicry or modeling of subtle and complicated chemical processes.[2] Such studies include those related to the elucidation of the mode of action of the natural photosynthetic reaction center[3] and those concerned with the handling and storage of information at the molecular level.[4] These two fascinating areas have experienced many outstanding advances over the years, from which a number of pertinent issues have arisen that may be usefully applied to monitor photoinduced intramolecular electron transfers,[5, 6] among other possible effects or functions.

Regarding artificial photosynthesis, a major goal is the controlled formation of long-lived photoinduced charge-separated states, which corresponds to the transient conversion of light into an electrochemical potential that may be used, under appropriate conditions, for energy storage or electricity production.[7] Such a process may be achieved within specially designed supramolecular architectures built-

[a] Dr. P. Lainé, Dr. E. Amouyal, Dr. F. Berruyer-Penaud
Laboratoire de Chimie Physique (CNRS UMR 8000)
Université Paris-Sud, Bâtiment 350
91405 Orsay Cedex (France)
Fax: (+33) 1-69-15-30-53
E-mail: philippe.laine@lcp.u-psud.fr

[b] Dr. F. Bedioui, V. Albin
Laboratoire d'Électrochimie et Chimie Analytique
(CNRS UMR 7575)
École Nationale Supérieure de Chimie de Paris
11 rue Pierre et Marie Curie, 75231 Paris Cedex 05 (France)

[**] Triarylpyridinium-Functionalized Terpyridyl Ligands for Photosensitized Supramolecular Architectures, Part 2. For Part 1 see reference [9].

  0947-6539/02/0814-3162 $ 20.00+.50/0

up of covalently linked electron-donating (D) and -accepting (A) subunits together with a photosensitizing chromophore (P).[5, 6a,c]

Within this framework, and in the course of our studies focussed on the design of new building blocks of potential interest for artificial photosynthesis and related research fields such as molecular electronics, we have proposed and synthesized[8, 9] a series of triarylpyridinium-derivatized terpyridyl molecules, $R^1{}_2R^2TP^+$-$(p)_n$tpy, as a new class of electron-acceptor-substituted ligands (A). When complexed with the d^6 transition-metal cations ruthenium(II) and osmium(II), the resulting polypyridyl chelates are intended to simultaneously play three key roles: 1) as structural assembling elements, 2) as efficient photosensitizers (P), and 3) as primary light-triggered electron donors within the generated multicomponent arrays (polyad systems). All complexes prepared to date[9] with the first members of the new family of ligands ($R^1 = R^2 = H$ and $n = 0, 1$), with or without a *p-N,N*-dimethylamino-phenylterpy moiety as an electron-donating ligand (D), are depicted here, along with their abbreviations nomenclature.

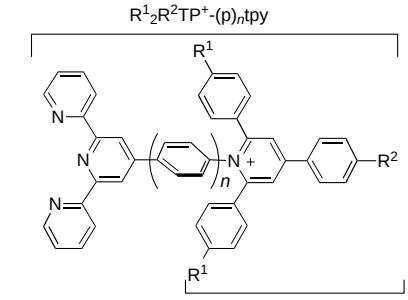

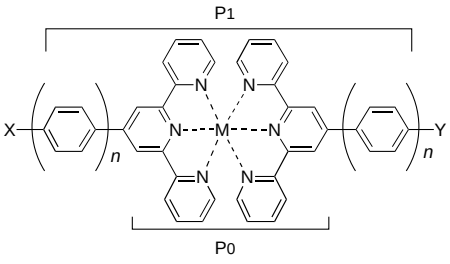

$n = 0$ and M = Ru^{II}		$n = 1$ and M = Ru^{II}, Os^{II}	
P0/M	X = Y = H	P1/M	X = Y = Me
P0A_2/M	X = Y = H_3TP^+	P1A_2/M	X = Y = H_3TP^+
P0A/M	X = H and Y = H_3TP^+	P1A/M	X = Me and Y = H_3TP^+
		D_2P1/M	X = Y = Me_2N
		DP1/M	X = Me_2N and Y = Me
		DP1A/M	X = Me_2N and Y = H_3TP^+

The salient features of these compounds are that they combine a well-defined topology (rigid structure) and a marked chemical flexibility (R^1 and R^2), allowing both a fine tuning of the properties of the electron-acceptor fragment and possible expansion of the supramolecular architectures (redox cascades, branched molecules).[8, 9]

To obtain further insight into the expected correlation between some of the intramolecular geometrical parameters and the photophysical behavior of the polyad systems reported herein, a detailed structural study was carried out.[9] It was shown that the actual conformation of the acceptor moieties (A) with respect to the connected photosensitizers (P), both in the solid-state (X-ray analysis) and in solution (NMR experiments), is such that there is almost no conjugation between these two components (see Figure 1), irrespective of whether P is P0 or P1.[9]

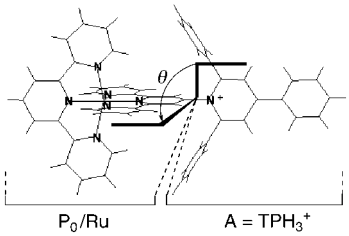

Figure 1. Pictorial representation of the "geometrical decoupling" ($\theta \approx 80-90^\circ$) between the photosensitizer and the acceptor components in the representative case of the P0A/Ru dyad (X-ray structure).[9]

This finding is crucial with regard to the nature and strength of the *intercomponent electronic coupling* within the polyad systems. This parameter is itself of great importance within the framework of the criteria that govern the formation of the targeted long-lived, charge-separated states, which are also those of supramolecular photochemistry.[4, 5, 6a,c] Therefore, beyond the thermodynamic and kinetic considerations, we specifically address this aspect in this paper. For a deeper understanding of the investigated photophysical behavior of these new photoactive supramolecular species, electrochemical and spectroelectrochemical experiments have been performed. These interrelated and complementary studies have allowed a rational explanation of the interesting photoinduced processes observed for this series of new compounds.

Results

Electrochemical properties: The electrochemical properties of organic model donor, acceptor, and associated ligands are gathered in Table 1. Salient electrochemical results for relevant reference compounds and polyad systems are collected in Table 2.

Ligands: Figure 2 shows cyclic voltammograms of H_3TP^+-p and its derivatives in acetonitrile that contains 0.1M $TBABF_4$ at a platinum disk electrode.

From the survey of the electrochemical data recapitulated in Table 1, it appears that:

1) The first and second reduction potentials of the H_3TP^+ systems are shifted towards less negative values on going from the model acceptor *N*-phenyl-2,4,6-triphenylpyridinium (H_3TP^+-p) to the tpy ligands, namely H_3TP^+-ptpy and H_3TP^+-tpy. Concomitantly, both electrochemical systems (single-electron processes) are seen to progressively merge together ($\Delta E_{1/2} = 160$ and 105 mV for H_3TP^+-p and

  0947-6539/02/0814-3163 $ 20.00+.50/0

Table 1. Electrochemical potentials of the organic ligands in acetonitrile + 0.1M $TBABF_4$ at a platinum electrode.[a]

	Me_2N-p	Me_2N-ptpy		H_3TP^+-p				H_3TP^+-ptpy			H_3TP^+-tpy
	$D^{+/0}$ (+ Dim.)	$D^{2+/+}$	$D^{+/0}$	$H_3TP^{3+/2+}$	$H_3TP^{2+/+}$	$H_3TP^{+/0}$	$H_3TP^{0/-}$	$H_3TP^{2+/+}$	$H_3TP^{+/0}$	$H_3TP^{0/-}$	$H_3TP^{+/-}$
E_{pa}	+0.80	+1.17	+0.93	+1.24	+1.05	−0.93	−1.08	+1.02	−0.92	−1.02	−0.85
E_{pc}	+0.57/+0.44	+1.10	+0.91	+1.00	+0.75	−1.01	−1.17	+0.86	−0.98	−1.09	−0.93
$E_{1/2}$	nd	+1.13	+0.92	+1.12	+0.90	−0.97	−1.13	+0.94	−0.95	−1.05	−0.89
n (rev)	nd (irr)	nd (irr)	1 (rev)	nd (irr)	1 (rev)	1 (rev)	1 (rev)	1 (rev)	1 (rev)	1 (rev)	2 (rev)

[a] E_{pa} and E_{pc}: anodic and cathodic peak potentials (vs SCE) measured by cyclic voltammetry at 0.2 Vs^{-1}; $E_{1/2}$/V (vs SCE) is calculated as $(E_{pa} + E_{pc})/2$; n is the number of electron involved in the electrochemical process; nd: not determined; rev: chemically reversible process; irr: chemically irreversible process.

Table 2. Electrochemical data of the examined complexes in acetonitrile + 0.1M $TBABF_4$ at Pt electrode.[a]

		$M^{III/II}$			$D^{+/0}$			$H_3TP^{+/0}$		
Entry		$E_{1/2}$	n	k°	$E_{1/2}$	n	k°	$E_{1/2}$	n	k°
1	P0/Ru	+1.31	1	4×10^{-3}	–	–	–	–	–	–
2	P0A/Ru	+1.44	1	7.8×10^{-3}	–	–	–	−0.77[b]	[b]	–
3	P0A_2/Ru	>+1.6	nd	nd	–	–	–	−0.78[b]	[b]	–
4	P1/Ru	+1.24	1	4×10^{-2}	–	–	–	–	–	–
5	P1A/Ru	+1.27	1	7.9×10^{-3}	–	–	–	−0.90	1	nd
6	P1A_2/Ru	+1.29	1	5.1×10^{-3}	–	–	–	−0.91	[c]	nd
7	DP1/Ru	+1.29	>1	nd	+0.93	1	1.7×10^{-2}	–	–	–
8	D_2P1/Ru	+1.37	>1	nd	+0.90	2	6.1×10^{-3}	–	–	–
9	DP1A/Ru	+1.29	1	2.6×10^{-3}	nd	nd	nd	−0.91	[d]	nd
10	P1/Os	+0.90	1	5.1×10^{-2}	–	–	–	–	–	–
11	P1A/Os	+0.93	1	1.7×10^{-2}	–	–	–	−0.91	[d]	nd
12	P1A_2/Os	+0.96	1	1.1×10^{-2}	–	–	–	−0.92	[c]	nd
13	DP1/Os	+0.82	1	>1	+1.05	1	3.8×10^{-2}	–	–	–
14	D_2P1/Os	+0.77	1	4.2×10^{-2}	+0.96	1	>1	–	–	–
					+1.12	1	1.3×10^{-2}			
15	DP1A/Os	+0.83	1	11×10^{-2}	+1.01	1	nd	−0.93	[d]	nd

		$H_3TP^{0/-}$			$P^{0/-}$			$P^{-/2-}$		
Entry		$E_{1/2}$	n	k°	$E_{1/2}$	n	k°	$E_{1/2}$	n	k°
1	P0/Ru	–	–	–	−1.23	1	nd	−1.48	1	nd
2	P0A/Ru	−0.77[b]	[b]	nd	−1.34	1	7.7×10^{-3}	nd	nd	nd
3	P0A_2/Ru	−0.78[b]	[b]	nd	nd	nd	nd	nd	nd	nd
4	P1/Ru	–	–	–	−1.24	1	2×10^{-2}	−1.47	1	1.4×10^{-2}
5	P1A/Ru	−1.00	1	nd	−1.25	1	9.2×10^{-3}	−1.50	1	7.9×10^{-3}
6	P1A_2/Ru	−0.98	[c]	nd	−1.31	1	4.7×10^{-3}	−1.54	1	3.0×10^{-3}
7	DP1/Ru	–	–	–	−1.24	1	1.3×10^{-2}	−1.48	1	3.5×10^{-3}
8	D_2P1/Ru	–	–	–	−1.29	1	8.5×10^{-3}	−1.50	1	5.7×10^{-3}
9	DP1A/Ru	−0.99	[d]	nd	−1.24	1	6.5×10^{-3}	−1.51[e]	1	nd
10	P1/Os	–	–	–	−1.20	1	3.1×10^{-2}	−1.47	1	2.4×10^{-2}
11	P1A/Os	−1.00	[d]	nd	−1.21	1	1.7×10^{-2}	−1.47	1	9.8×10^{-3}
12	P1A_2/Os	−0.99	[c]	nd	−1.25	1	1.2×10^{-2}	−1.52	1	2.2×10^{-2}
13	DP1/Os	–	–	–	−1.22	1	2.3×10^{-2}	−1.48	1	7.6×10^{-3}
14	D_2P1/Os	–	–	–	−1.24	1	2×10^{-2}	−1.50	1	7.9×10^{-3}
15	DP1A/Os	−1.02	[d]	nd	−1.23	1	4.7×10^{-2}	−1.49	1	1.9×10^{-2}

[a] $E_{1/2}$ [V] (vs SCE) is calculated as $(E_{pa} + E_{pc})/2$, in which E_{pa} and E_{pc} are the anodic and cathodic peak potentials, respectively, measured by cyclic voltammetry at 0.2 Vs^{-1}; n is the number of electrons involved in the redox process determined by hydrodynamic voltammetry by comparison with reference components; k° [cms^{-1}] is the standard rate constant for an electron-transfer reaction; –: not present in the complex; nd: not determined. [b] $H_3TP^{+/0}$ cathodic wave merges with $H_3TP^{0/-}$ (one 1+1 or 2+2 electron unresolved wave). [c] $H_3TP^{+/0}$ cathodic wave merges with $H_3TP^{0/-}$ (one 2+2 electron partially resolved wave). [d] $H_3TP^{+/0}$ cathodic wave merges with $H_3TP^{0/-}$ (one bielectronic partially resolved wave). [e] $E_{1/2}$ determined by hydrodynamic voltammetry.

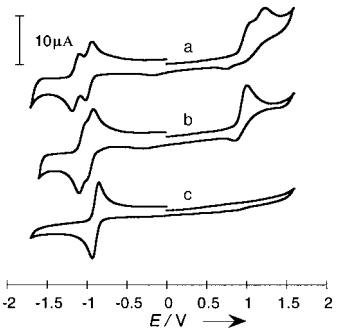

Figure 2. Cyclic voltammograms for a) H_3TP^+-p ($c = 4.7\times10^{-4}$M), b) H_3TP^+-ptpy ($c = 5.1\times10^{-4}$M), and c) H_3TP^+-tpy ($c = 3.5\times10^{-4}$M) in CH_3CN + 0.1M $TBABF_4$ (Pt electrode, $v = 200$ mVs^{-1}).

H_3TP^+-ptpy, respectively) to give a single two-electron process for H_3TP^+-tpy. As expected, the redox properties of the pyridinium moiety are influenced by its peripheral substituents.[10, 11] This sensitivity clearly shows that the *N*-substituents such as pyridine (from tpy) and phenyl (from the spacer) can also be considered as a means of tuning the properties of the pyridinium ring.

2) A reversible electrochemical oxidation process is observed at +0.90 V for the model acceptor H_3TP^+-p and at +0.94 V for the associated phenylterpy derivative (H_3TP^+-ptpy), but is not seen for H_3TP^+-tpy nor for the complexes. In view of the fact that the first reduction

  0947-6539/02/0814-3164 $ 20.00+.50/0 *Chem. Eur. J.* **2002**, *8*, No. 14

potential of H_3TP^+ within H_3TP^+-tpy is very close to that of the acceptor moiety in H_3TP^+-ptpy complexes with Ru^{II} and Os^{II} (Table 2), it is not surprising that the organic dication is not formed within these complexes in the investigated potential range. The reason is that the coordinative bonding of the covalently linked tpy to the transition metal ion shifts its oxidation potential towards higher energy, in the same manner as the direct replacement of an *N*-phenyl group by a pyridine moiety increases the oxidation potential of the pyridinium.

3) In the case of H_3TP^+-p, an additional irreversible oxidation process is observed at +1.12 V. These oxidation processes may be related to the formation of a radical dication and trication for H_3TP^+-p, as previously suggested for pyrylium[12] and diazobenzoperylene moieties.[13]
4) Regarding the *p*-amino-derivatized species, an irreversible anodic process is observed for the *N*,*N*-dimethylaniline model donor at +0.8 V, while a reversible oxidation reaction is observed for the associated ligand at +0.92 V. In the latter case, the attached tpy groups prevent the *N*,*N*-dimethylanilino radical cation from undergoing the well-known *para*-oriented homocoupling (dimerization) that takes place in the case of the *N*,*N*-dimethylaniline compound.[14] The reversibility of the first oxidation reaction (radical monocation formation) of the amino derivative is then restored. The radical dication can also be obtained at higher potentials, although it is not stable.

Complexes: On the basis of the electrochemical data collected for organic reference species and ligands (Table 1), the main electrochemical features of the related coordination compounds (Table 2) can be straightforwardly assigned by analogy. A general trend is the sizable electrochemical perturbation within the polyad systems of both the organic and metal-based subunits with respect to their isolated parent species. When complexed, acceptor ligands are easier to reduce, while donor ligands are more difficult to oxidize. Accordingly, the metal-centered redox potentials, especially for the oxidation process, are sensitive to whether the tpy ligand bears a stabilizing electron-releasing or a destabilizing electron-withdrawing group. However, some differences in behavior exist between the various systems examined; these are reminiscent of some more basic features regarding intercomponent electronic coupling.[6a,c] A thorough analysis of the electrochemical results is thus required. To illustrate the electrochemical behavior of the investigated polyads, Figures 3–6 show typical cyclic voltammograms of selected dyads and triads in acetonitrile solution.

P0A, P1A, P0A_2, and P1A_2 reference dyads and triads: The redox processes related to the metal-centered P0 and P1-based polyad systems show differences due to the presence of the H_3TP^+ acceptor group. Within the P0 series, attachment of this acceptor results in a dramatic incremental anodic shift of the $Ru^{II/III}$ potential of about +140 mV per additional H_3TP^+ unit (Table 2, entries 1–3). This value drops to +30 mV within the P1 family, irrespective of whether M is Ru or Os (Table 2, entries 4–6 and 10–12). The effect of the presence of the acceptor group is also manifested in a decrease in the standard rate constant k° of the $M^{II/III}$ electron-transfer process (Table 2, entries 4–6 and 10–12). This phenomenon can be rationalized in terms of a strengthening of the acceptor moiety in the P0 series (*vs.* P1) and can be viewed as further evidence of the above mentioned tuning effect of the electrochemical properties of H_3TP^+ from those observed for the free ligands. Indeed, a combined anodic shift and merging of the pyridinium first and second reduction processes is clearly evident on comparing the data for the homoleptic ruthenium complex P1A_2/Ru with those for P0A_2/Ru (Table 2, entries 3 and 6).

With regarding to the P0-based compounds, the strong interaction between the acceptor group and the photosensitizer also becomes apparent when considering the first ($P^{0/-}$) and second ($P^{-/2-}$) reduction processes related to the tpy ligands (Figure 3).

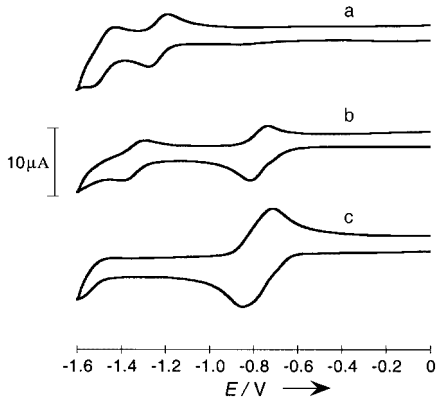

Figure 3. Cyclic voltammograms for a) P0/Ru ($c = 2.6 \times 10^{-4}$ M), b) P0A/Ru: ($c = 2.65 \times 10^{-4}$ M), and c) P0A_2/Os ($c = 2.5 \times 10^{-4}$ M) in CH_3CN + 0.1M $TBABF_4$ (Pt electrode, $v = 200$ mVs^{-1}).

In the case of the heteroleptic P0A/Ru complex, once the acceptor has been reduced, the electron density located in direct proximity to the chromophore is so high that the reduction of tpy ligands, which corresponds to the addition of a third or even a fourth electron to the complex, is disfavored and cannot be fully achieved in the examined potential range (up to −1.6 V). With respect to the homoleptic P0A_2/Ru complex, the effect of the primary reduction processes of both acceptor groups (four-electron process) on those of P0 is more dramatic, such that P0 cannot be subsequently reduced (Table 2, entries 1–3). The presence of the acceptor group is also manifested in a decrease in the standard rate constants k° of the $P^{0/-}$ and $P^{-/2-}$ electron-transfer processes (Table 2, entries 4–6 and 10–12).

Finally, it is worth noting that, in contrast to what is seen for the P0/Ru series, the reduction processes of the complex photosensitizer are achieved for both the P1/Os and P1/Ru analogues, as is clearly illustrated in Figure 4.

In conclusion, it can be stated that the observed differences in the oxidation and reduction behavior of the P0- and P1-based acceptor polyad systems indicate that these compounds belong to different categories from the point of view of the definition of supramolecular (photo)chemistry.[4, 5, 6a,c]

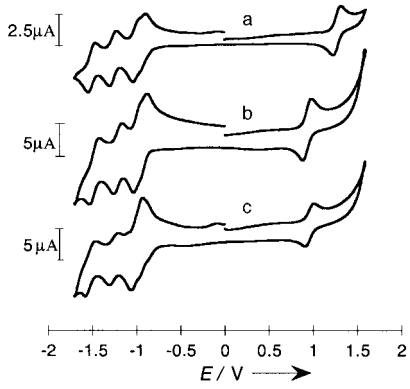

Figure 4. Cyclic voltammograms for a) P1 A/Ru ($c = 2.4 \times 10^{-4}$ M, $v = 200$ mVs^{-1}), b) P1 A/Os ($c = 2.4 \times 10^{-4}$ M, $v = 300$ mVs^{-1}), and c) P1 A_2/Os ($c = 2.25 \times 10^{-4}$ M, $v = 300$ mVs^{-1}) in CH_3CN + 0.1 M $TBABF_4$ (Pt electrode).

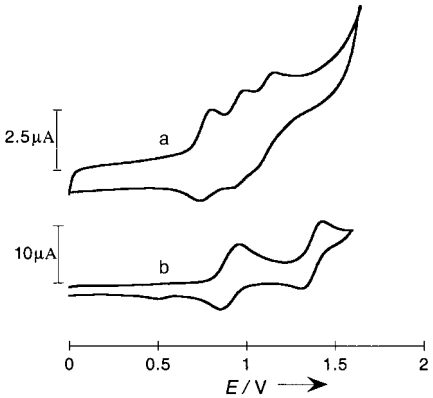

Figure 5. Cyclic voltammograms for a) D_2P1/Os ($c = 1.7 \times 10^{-4}$ M) and b) D_2P1/Ru ($c = 4.3 \times 10^{-4}$ M) in CH_3CN + 0.1 M $TBABF_4$ (Pt electrode, $v = 200$ mVs^{-1}).

DP1 and D_2P1 reference dyads and triads: In contrast to the H_3TP^+ derivatives of the P1 family, donor-bearing complexes exhibit strong modifications of their electrochemical properties as compared to those of the parent species.

For the Ru^{II} series, the redox potentials related to the metal-centered oxidation are rather close to that of the irreversible second oxidation process of the dimethylamino group in the Me_2N-ptpy parent species (+1.13 V, Table 1). Thus, this latter oxidation process cannot be observed in the polyad systems. This perturbation was also evident from the shapes of both the cyclic and hydrodynamic voltammograms, which showed more than one electron to be involved in the $Ru^{II} \rightarrow Ru^{III}$ oxidation process of the DP1/Ru and D_2P1/Ru species, in contrast to the oxidation of the P1/Ru complex. Such behavior is indicative of an electrocatalyzed reaction at the potential of the metal-centered oxidation process.[15]

In the case of the osmium compounds, several particular features have been observed:

First, it appears that, similarly to what was seen with the ruthenium analogues, for the *second* irreversible oxidation of D, the metal-centered oxidation process of P1/Os and the *first* reversible oxidation process of Me_2N- (in Me_2N-ptpy) occur at very close potentials: +0.90 V and +0.92 V, respectively. Thus, in the case of the DP1/Os complex, the redox process at +0.82 V is related to the one-electron metal-centered oxidation reaction, which is made easier by the presence of the electron-rich and conjugated dimethylamino group; the displacement is about −80 mV relative to that of the parent P1/Os. The second process at +1.05 V is consequently related to the amino-centered oxidation, the potential being shifted to a more positive value (by about +135 mV) relative to that of the first oxidation process of Me_2N-ptpy. This is due to the fact that both its complexation with the transition metal cation and the primary oxidation of the latter reduce the electron density of the donor subunit such that it becomes more difficult to oxidize. Note that the presence of D also leads to an increase in the standard rate constant k° of the $Os^{II/III}$ electron-transfer process when P1/Os is compared to DP1/Os (Table 2, entries 10 and 13).

Second, a splitting of the donor-centered redox processes within the homoleptic D_2P1/Os complex is observed (Figure 5 and Table 2: entries 10, 13, and 14). This suggests that the three components of the complex behave as strongly electronically and electrostatically coupled elements. The oxidation process occurring at the less positive potential (+0.77 V) is related to the metal-centered one. Its potential value corresponds to a stabilization energy of Os^{III} of +0.13 eV as compared to that of the parent compound P1/Os (and of +0.05 eV compared to DP1/Os). The two other distinct higher potential processes, occurring at +0.96 V and +1.12 V, are related to the two nonequivalent electron-releasing D substituents. Note that the average value of these two D-centered oxidation potentials (+1.04 V) is very close to that of the oxidation potential related to D within the DP1/Os dyad (+1.05 V). The unexpected loss of degeneracy of the two chemically identical donor moieties originates from their strong interaction, even though they are not directly connected. Hence, it seems that the transition metal cation plays the role of a relay or coupling element. The initial formal oxidation of one of the two donors destabilizes the other D-redox center, in the same way as strongly coupled components would be in a mixed-valence species.[16]

Finally, by comparing the electrochemical behavior of D_2P1/Os with that of D_2P1/Ru (Figure 5), it appears that no splitting of the oxidation wave related to $D^{0/+}$ is observed in the case of the ruthenium complex: both donor substituents are oxidized at the same potential in one two-electron process at +0.90 V, as predicted for independent and identical redox couples. Indeed, the $Ru^{II/III}$ redox process occurs at significantly higher potential than that of $D^{0/+}$, and thus Ru^{III} cannot act as a relay. Nevertheless, the ruthenium-based photosensitizer was expected to exhibit some modification of its oxidation potential due to the presence of the conjugated electron-releasing groups, similar to that detected for the osmium series. For the reasons outlined at the beginning of this section, that is, intermingled redox processes occurring at the $D^{+/2+}$ and $Ru^{II/III}$ potentials, this was not actually the case.

DP1 A triads: As is apparent from a careful inspection of the data in Table 2, and as depicted in Figure 6, the electrochemical behavior of the DP1 A/Os triad system can best be viewed as a superposition of the behavior of the model dyads described above rather than as simply the sum of those of the

  0947-6539/02/0814-3166 $ 20.00+.50/0 *Chem. Eur. J.* **2002**, *8*, No. 14

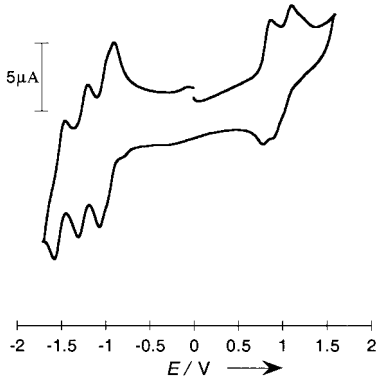

Figure 6. Cyclic voltammogram for DP1 A/Os ($c = 2.55 \times 10^{-4}$ M) in CH_3CN + 0.1 M $TBABF_4$ (Pt electrode, $v = 400$ mVs^{-1}).

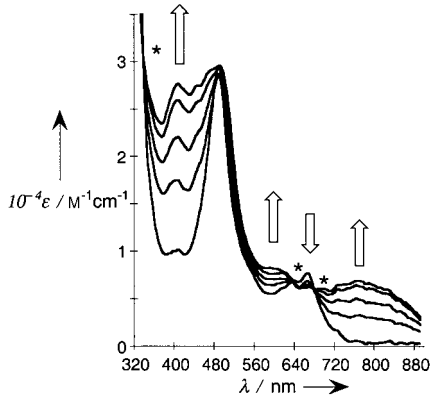

Figure 7. Spectral changes observed during the reduction of P1/Os at -1.2 V in CH_3CN (0.1 M $TBABF_4$). *: isobestic point.

various individual model components D, P1, and A. More precisely, these findings suggest that the electrochemical features of DP1A triads are those of the corresponding donor dyads DP1 plus that of A (A being very weakly coupled with P1 within P1A). The DP1 A/Ru triad shows similar behavior.

Spectroelectrochemical properties: To further identify the characteristic signatures of the activated species generated in the excited state, and especially that of the reduced acceptor $[A]^-$ resulting from photoinduced intramolecular electron transfer, selected ground-state absorption spectra of both the reduced H_3TP^+ and P1/Os entities, as well as that of the acceptor dyad P1 A/Os, were recorded. These spectroelectrochemistry experiments were performed at controlled potentials in acetonitrile that contained 0.1 M $TBABF_4$.

Among the three triphenylpyridinium-derivatized organic molecules at our disposal, only the model acceptor H_3TP^+-p exhibits two well-separated single-electron waves (see Figure 2) that allow the reduction process to be finely monitored. The one-electron reduction of the model acceptor at -1 V allows the spectrum of H_3TP^0 to be recorded, which features one broad absorption band at 503 nm (Table 3).

Table 3. Summary of absorption maxima of reduced and oxidized key species.

	λ_{max} [nm] (ε [10^4 M^{-1}cm^{-1}])			
$[(Me\text{-}ptpy)Os^{II}(ptpy\text{-}Me^-)]^+$	406	505	600	760
H_3TP^0-p		503 (0.57)		
H_3TP^0 within [P1 A/Os]$^-$	360	522		
$[(Me\text{-}ptpy)_2Os^{III}]^{3+}$ [a]	407 (2.27)	523 (0.545)	618 (0.395)	

[a] Ref. [17].

Controlled reduction of the model photosensitizer P1/Os at -1.2 V results in a clean one-electron reduction process, which was followed by recording the UV/Vis absorption spectra shown in Figure 7. These spectra exhibit three isobestic points at around 340, 640, and 680 nm. The relative abundance, α, of the two species [P1/Os] and $[P1/Os]^-$ can therefore be calculated using Equation (1), with $\alpha = [P1/Os]^-/[P1/Os]$, $n = 1$, and $\Delta E = (E_{applied} - E_{1/2}[P1/Os]^{0/-})$:

$$RT\ln\alpha = nF\Delta E \quad (1)$$

The electronic spectrum of the reduced $[P1/Os]^-$ chromophore could then be determined (Table 3). In the case of the acceptor unit involved in the acceptor-based dyad, the monoreduced species cannot be obtained in pure form owing to its intrinsic electrochemical properties (almost merged waves for the two monoelectronic reductions of the acceptor moiety). Indeed, the spectra obtained in the course of electrochemical reduction of the acceptor dyad P1 A/Os at -1.0 V (Figure 8) show complicated features. By comparison with the spectra of

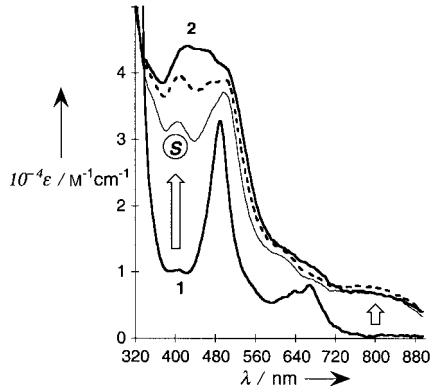

Figure 8. Spectral changes observed during the reduction of P1 A/Os at -1 V in CH_3CN (0.1 M $TBABF_4$). 1) Before the electrolysis. 2) End of the electrolysis. S) Selected intermediate absorption spectrum.

the reduced P1/Os at -1.2 V (Figure 7), the electronic features of the reduced dyad exhibit some intriguing similarities. Specifically, a pronounced increase in the absorption at around 400 nm and in the NIR region (beyond 700 nm) is observed, since the reduction of the inorganic core is not expected to occur at -1 V. One should also note the evident broadening that accompanies the apparent enhancement of the absorption band originally situated at 491 nm (which is concomitantly red-shifted by about 10 nm) and the absence of the previously observed isobestic points. These two features clearly indicate that the reduction of P1 A/Os at -1 V involves at least three different absorbing species, one of which is the previously characterized $[P1/Os]^-$ chromophore.

As has been reported previously,[9] the electronic features of P1/Os (^{1}MLCT and ^{3}MLCT transitions) are largely indepen-

dent of whether the photosensitizer is isolated or belongs to an acceptor dyad or triad (i.e., whether it is linked to one or two H_3TP^+ UV-absorbing subunits). Thus, on the basis of the absorption in the *visible region*, one can reasonably state the following formal equivalences for the chromophore species: [P1 A/Os] = [P1/Os] and [P1 A/Os]$^-$ = [P1/Os] + [A]$^-$. However, when the reduction is incomplete (spectrum S, Figure 8), the solution formally contains only a mixture of P1 A/Os and [P1 A/Os]$^-$ compounds. As is evident from Figure 8 and as noted above, the electron added to the acceptor moiety [A]$^-$ is partially delocalized over the photosensitizer, which allows the formal existence of the [P1/Os]$^-$ chromophoric species. The postulated equivalence concerning the reduced species must then be corrected as follows: [P1 A/Os]$^-$ = [P1/Os] + [A]$^-$ + [P1/Os]$^-$, and in this way the critical number of three chromophores is reached. In view of the fact that chromophoric components behave in an independent manner and that the only absorbing species in the visible region are P1/Os, [P1/Os]$^-$, and [A]$^-$, one can assume that the spectrum S is the sum of the weighted absorption contributions of these three chromophores. Moreover, the only absorbing species at 800 nm is the reduced [P1/Os]$^-$ chromophore within [P1 A/Os]$^-$. Thus, it is possible to deduce the electronic features of the reduced acceptor [A]$^-$ within the dyad, with the help of the relationship that accounts for the conservation of P1/Os-based entities. The relative contributions to spectrum S of the identified chromophores are depicted in Figure 9, which shows the extracted profile of [A]$^-$ within [P1 A/Os]$^-$. Absorption maxima of these reduced species, together with that of the chemically oxidized reference photosensitizer P1/Os, are gathered in Table 3. Apart from that of [P1/Os]$^+$, the reported molar extinction coefficients of the reduced species are only estimates and are given for illustrative purposes only. It is noteworthy that the bathochromic shift ($\Delta E \approx 0.09$ eV) of the absorption band of H_3TP^0 on going from the isolated model entity to the acceptor component embedded within the corresponding dyad is consistent with their related electrochemical behavior (Tables 1 and 2). Thus, the first reduction potential of H_3TP^+ is shifted from -0.97 V to the less negative potential of -0.91 V, which corresponds to a stabilization energy of about 0.06 eV.

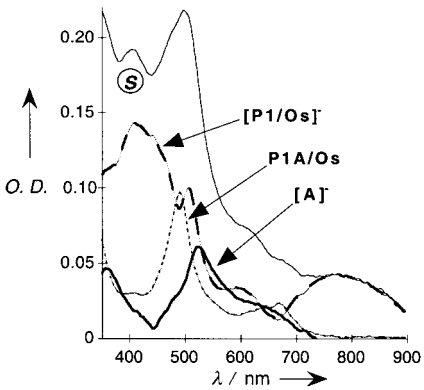

Figure 9. Weighted contributions of P1 A/Os, [P1/Os]$^-$, and [A]$^-$ chromophore species to the absorption spectrum S.

Photophysical properties: Luminescence properties of the Ru^{II} and Os^{II} bis(terpyridyl) complexes offer a suitable means of probing intramolecular processes such as photoinduced electron-transfer (PET). Furthermore, comparison between room- and low-temperature photophysical behavior helps in distinguishing the various possible mechanisms that may account for the observed photoinduced processes. The photophysical properties of the polyad species were therefore determined at both 293 K and 77 K (frozen matrix). Data for P0- and P1-based series of compounds, along with some significant informative parameters, are collected in Tables 4 and 5.

Radiative, k_r [Eq. (2)], and nonradiative, k_{nr} [Eq. (3)], rate constants,[18, 19] as well as excited-state redox potentials

$$k_r = \Phi_{em}/\tau \quad (2)$$

$$k_{nr} = (1 - \Phi_{em})/\tau \quad (3)$$

Table 4. Photophysical data for P0-based compounds.

	293 K[a]					77 K[b]			
	λ_{max} [nm]	τ [ns]	Φ_{em}	k_r [s^{-1}]	k_{nr} [s^{-1}]	λ_{max} [nm]	τ [μs]	E(III/II*) [V]	E(II*/I) [V]
P0/Ru	629[c]	0.56[d]	$\leq 5 \times 10^{-6}$ [c]	$\leq 8.9 \times 10^3$	$\geq 1.8 \times 10^9$	598, 645 sh	10.0	−0.76	+0.84
P0 A/Ru	670	55	7.3×10^{-4}	1.3×10^4	1.8×10^7	636, 687 sh	8.8	−0.51	+0.61
P0 A_2/Ru	644	27	3.9×10^{-4}	1.4×10^4	3.7×10^7	622, 672 sh	10.6	nd	nd

[a] In acetonitrile. [b] In butyronitrile; sh: shoulder. nd: not determined. [c] Ref. [21]. [d] Ref. [22].

Table 5. Photophysical data for P1-based compounds.

	293 K[a]					77 K[b]			
	Ru-based	Os-based				Ru-based		Os-based	
	τ [ps]	λ_{max} [nm]	Φ_{em} ($\times 10^2$)	I_{em}rel [%]	τ [ns]	λ_{max} [nm]	τ [μs]	λ_{max} [nm]	τ [μs]
P1	580	734	2.00	100	247	627, 684 sh	11.65	720, 790 sh	3.05
P1 A	740	750	1.02	50.9	168	632, 691 sh	11.72	721, 790 sh	2.7
P1 A_2	820	743	1.52	76.3	222	631, 690 sh	12.14	722, 795 sh	2.8
DP1	490	747	1.48	74.3	206	641, 696 sh	14.19	728, 797 sh	2.2
D_2P1	460	753	1.61	80.5	212	650, 708 sh	14.50	756	1.7
DP1 A	510	764	0.24	12.1	57	640, 695 sh	11.60	758	2.0

[a] In acetonitrile. [b] In butyronitrile. sh: shoulder.

0947-6539/02/0814-3168 $ 20.00+.50/0 *Chem. Eur. J.* **2002**, *8*, No. 14

E(III/II*) [Eq. (4)] and E(II*/I) [Eq. (5)],[18–20] have been calculated according to the literature, assuming that the quantum yield for the triplet state formation is unity, as is usually the case for polypyridine complexes of Ru^{II},[18] where E_{em}(0-0) is E_{em} at 77 K.:

$$E(\mathrm{III/II^*}) = E_{1/2}(\mathrm{M^{III/II}}) - E_{em}(0\text{-}0) \quad (4)$$

$$E(\mathrm{II^*/I}) = E_{1/2}(\mathrm{P^{0/-}}) + E_{em}(0\text{-}0) \quad (5)$$

Room-temperature luminescence properties: It is clear from the obtained data that, in acetonitrile, the P0-based compounds exhibit rather good luminescence properties with easily measurable emission lifetimes of a few tens of nanoseconds, whereas the isolated photosensitizer itself, P0/Ru, does not emit (Table 4). Typical luminescence spectra of P0-based polyad systems are shown in Figure 10.

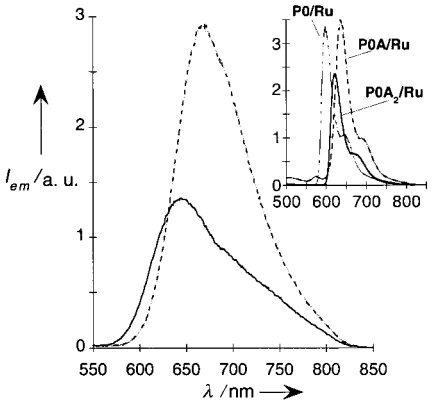

Figure 10. Luminescence spectra (room temperature, isoabsorptive deoxygenated acetonitrile solutions at $\lambda_{exc.} = 450$ nm, uncorrected) of P0A/Ru (dashed) and P0A_2/Ru (solid). Inset: uncorrected luminescence spectra in butyronitrile rigid matrix at 77 K of P0/Ru (dashed-dotted), P0A/Ru (dashed), and P0A_2/Ru (solid).

For the P1-based compounds, two trends are observed depending on the nature of the transition metal cation involved. For the ruthenium complexes, subnanosecond phosphorescence lifetimes are enhanced by about 30 and 40% for P1A/Ru and P1A_2/Ru, respectively, as compared to that of the model photosensitizer, whereas the opposite trend is observed for the donor-based polyads. For the osmium complexes, which are strongly luminescent, all the examined polyad systems exhibit an attenuation of their luminescence properties relative to those of the reference photosensitizer, irrespective of whether electron-withdrawing or -releasing ligands are involved. These divergent general trends are in fact typical of Ru and Os complexes.[6a,c] However, for the osmium-based compounds, it is worth noting that donor-group-bearing polyads (DP1/Os and D_2P1/Os) that emit at the same or lower energy than the acceptor dyad do exhibit longer luminescence lifetimes. This indicates that the energy-gap law does not fully account for the attenuation effect observed for P1A/Os.

Low temperature emission properties: At low temperature (in the rigid matrix of frozen butyronitrile), all the complexes are strongly luminescent and show the classical blue shift of their emission band maxima relative to that observed at room temperature (fluid medium). However, some discrepancies are observed depending on 1) the nature of the photosensitizer, P0 or P1, and 2) whether P1 is linked to D and/or A in the P1 series. Polyads composed only of P1 and A components show photophysical features very similar to those of their respective reference photosensitizers (P1/Ru and P1/Os). This is no longer true for P0-based acceptor polyad systems or for P1-based donor dyads and triads. Indeed, all of these exhibit red-shifted emission bands and significantly modified luminescence lifetimes. Moreover, in the case of P1 and D being connected, a further distinction has to be made between Ru^{II} complexes, which display enhanced phosphorescence lifetimes with respect to P1/Ru, and the Os^{II} analogues, which display shorter lifetimes than P1/Os. Nevertheless, despite the difference in sensitivity of the photophysical properties of P1-based complexes, depending on the nature of both their covalently attached neighbors (D and/or A) and their constituent transition-metal cation (Ru or Os), the luminescence behavior of the entire P1-based series of polyads can be rationalized in terms of the classical energy-gap law. This correlation between the emission lifetime originating from the lowest triplet excited state (^{3}MLCT) of each complex at low temperature and the energy of this latter emitting state at 77 K (E_{em}(0-0)) is illustrated in Figure 11.[23]

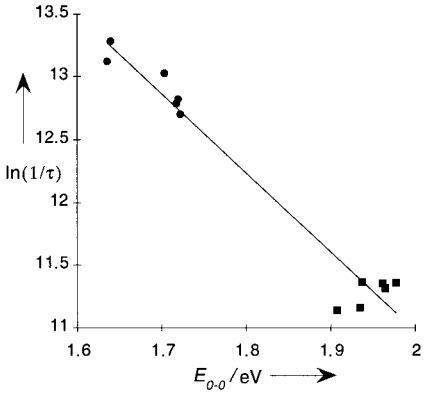

Figure 11. Correlation of $\ln(1/\tau)$ with ^{3}MLCT emission energy E_{em}(0-0) for the P1 series of complexes (slope $= -6.29$, $R = 0.98$). Ru^{II} species (solid squares), Os^{II} complexes (solid circles).

It is also well known that a linear correlation can be expected between the energy of the emission maximum (at 77 K) and the difference ($\Delta E_{1/2}$) between first oxidation and reduction potentials of the complexes, $E_{1/2}(\mathrm{M^{III/II}})$ and $E_{1/2}(\mathrm{P^{0/-}})$, respectively. Once again, the points, particularly those corresponding to the Ru series, are scattered, but a linear correlation can be found for the whole Ru and Os series of complexes of the P1 family, with a slope of 0.54 and an intercept of 0.56 (correlation coefficient 0.967). This correlation is very similar to that reported by Maestri et al.[21] (slope $= 0.64$, intercept $= 0.41$) for the other series of Ru^{II} tpy complexes bearing electron-accepting and -donating substituents mentioned above.

From these results, it appears that the Ru series is more sensitive to the substituents of the ligands than the Os series. Such complications are generally ascribed[20a] to accessible

low-lying dd states above the ^{3}MLCT emitting level, which greatly affect the photochemical stability and the MLCT excited-state lifetime of the Ru^{II} complexes.

Excited-state absorption properties: Transient absorption spectra were recorded at room temperature for the polyad systems incorporating only the P1 chromophore. With the exception of the P1 A/Os complex, which was studied in greater detail as it appeared to be the most likely to undergo an intercomponent PET, the overall behavior of the two series of compounds (Ru and Os) proved to be qualitatively very similar to that of their related photosensitizer. The only sizable perturbations were found to originate from substituent effects when D was involved.

For comparison purposes, transient absorption spectra of the reference photosensitizer P1/Os were recorded at different times after the excitation pulse, under the same experimental conditions as used for the acceptor dyad. Besides the expected variations in the proportions of their different features, which are reminiscent of the respective ground-state electronic properties of P1/Os and P1 A/Os, the transient absorption difference spectra (Figure 12) clearly show the following significant differences:

1) Of the strong positive absorption features located at around 390 and 600 nm for the model photosensitizer P1/Os, which are usually ascribed to the reduced ligand $[Me\text{-}ptpy]^-$,[6c, 17] the latter (in the visible region) is clearly diminished in the transient absorption difference spectrum of P1 A/Os, while the former (in the UV) corresponds to a minimum.
2) In both cases, the expected pronounced bleaching band at 490 nm corresponding to the depopulation of the ^{1}MLCT ground state is observed, accompanied by the correlated formation of the osmium-centered oxidized photosensitizer, as manifested in the positive absorption at about 430 nm.[6c, 17] However, one may note the rather uneven yet reproducible profile of the bleaching band of the acceptor dyad, with a shoulder at lower energy (at about 510 nm), compared to that of the isolated reference photosensitizer, which is well-shaped and much more intense.
3) Concerning the CT states, one may also note that the clearly detected bleaching in the 650 – 680 nm region for P1/Os, associated with the disappearance of the ground-state ^{3}MLCT band,[17] is observed with the same order of magnitude for P1 A/Os.
4) Regarding the features in the UV region of the spectra, a positive absorption maximum that is not present in the spectrum of P1/Os 20 ns after the laser excitation, is detected at 360 nm for P1 A/Os.

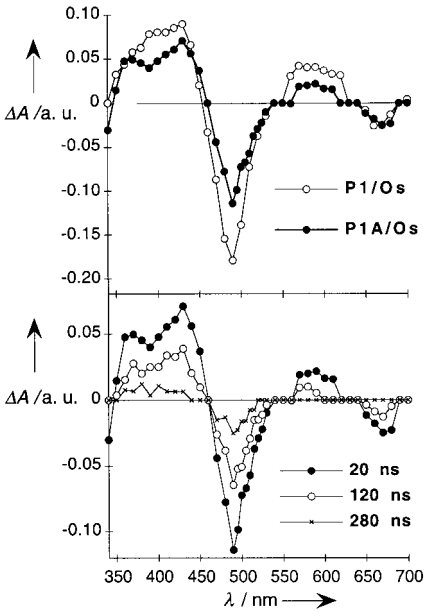

Figure 12. Comparative transient absorption difference spectra of P1/Os and P1 A/Os observed at 20 ns for isoabsorptive acetonitrile solutions at $\lambda_{exc.} = 308$ nm (top), and transient absorption difference spectra of P1 A/Os at the times indicated following the 10 ns laser flash (bottom).

Discussion

Intercomponent coupling: The electrochemical properties of the P1/A-based compounds parallel the previously reported ground-state electronic behavior[9] in that they are found to be scarcely perturbed with respect to those of the isolated parent species. These features are of the same order of magnitude as those measured for a P1 photosensitizer connected through a saturated methylene spacer to a strong electron acceptor such as methyl viologen, MV^{2+} (these two components being considered as not electronically coupled).[6a,c, 17, 24] On the contrary, regarding the electrochemical behavior of complexes with dimethylamino-modified ligands (P1/D family) and with directly acceptor-substituted ligands (P0 series), both donor-stabilized and acceptor-destabilized metal-centered oxidation potentials as well as noticeable perturbations of D/A ligand-centered redox processes were evidenced, these also being consistent with the previously reported ground-state electronic properties.[9] In the present case, this expected correlation[6a,c, 21] reflects significant intercomponent couplings.

Further insights into these electronic couplings could also be gained from spectroelectrochemistry experiments. The initial and principal aim of this study was to determine the electronic signature of the reduced acceptor within the polyad systems, to allow comparisons with the results obtained from laser flash photolysis experiments, in particular transient absorption spectroscopy. However, a prerequisite for the spectroelectrochemistry to be meaningful is that only weakly coupled chromophoric components are involved within the investigated supramolecular assemblies, which is a priori the case for P1 A and P1 A_2 reference dyads and triads. Among these polyads, the P1 A/Os species was studied in greater detail owing to its photophysical and thermodynamic features (see below), these being compatible with the occurrence of intramolecular PET leading to the target charge-separated state ($P1^+ - A^-$). Assuming almost independent electrochemical behavior of the electroactive subunits within the Os^{II} acceptor dyads P1 A/Os, it was possible to calculate the difference absorption spectrum of a partially reduced P1 A/Os solution (spectrum S in Figure 9), in other words, to subtract the various identified contributions attributable to the isolated reduced parent species. Indeed, and as expected, the

  0947-6539/02/0814-3170 $ 20.00+.50/0 *Chem. Eur. J.* **2002**, *8*, No. 14

calculated spectrum (Figure 9) was very similar to that of the monoreduced model acceptor H_3TP^0-p, showing a slight bathochromic shift of about 0.1 eV with respect to the other model species. This difference spectrum could be ascribed to $[A]^-$, and the stabilization energy was found to be in accordance with the slight modification of the redox properties measured for A when connected to P1. Noteworthy observations are that 1) P1 A/Os could be successfully investigated by spectroelectrochemistry, and 2) the unique features of H_3TP^0 were recovered, as they constitute the a posteriori confirmation that the acceptor moiety does behave independently of the photosensitizer subunit. Accordingly, the fact that the three different species responsible for the spectrum S can be related to model chromophoric compounds (P1/Os, $[P1/Os]^-$, $[A]^-$), but not to other or unknown chromophores, further confirms that components within the dyad interact weakly. This really fulfils the requirements of supramolecular photochemistry.[5, 6a,c, 25]

Hence, taken together with the previously reported structural and ground-state electronic features,[9] the main points that emerge from the observed electrochemical and spectroelectrochemical behavior are that:

1) In spite of their sharply twisted arrangement, A and P0 exert a mutual influence on each other (substituent effect) such that A has to be considered as being strongly electronically coupled to P0.
2) The combined effects of their "geometrical decoupling" (orthogonal conformation)[9] and the intrinsically weak electron-withdrawing properties of the H_3TP^+ unit, together with the attenuating contribution of the phenyl as a spacer, result in A and P1 being weakly coupled components.
3) D is strongly coupled to P1.

Consequences for photophysical behavior and PET phenomena: The light excitation of photosensitized molecules (absorption) provides a means of inducing intramolecular processes such as PET, whereas the light collected from molecular systems (emission) provides an informative means of probing the intramolecular response to previous electromagnetic stimuli. Steady-state and time-resolved photophysical experiments were therefore performed on the various photosensitized polyad systems in order to characterize their properties and to assess their ability to undergo PET with possible CS states.

Room temperature luminescence of the P0 family: At room temperature, one should note that 1) a lower energy for the ^{3}MLCT level is not related to a shorter luminescence lifetime, 2) radiative rate constant values are the same for P0 A_2/Ru and P0 A/Ru, whereas the nonradiative decay appears to be about half as efficient for P0 A/Ru as it is for P0 A_2/Ru (Table 4), and 3) the ^{3}MLCT level is lower in energy for P0 A/Ru than it is for P0 A_2/Ru. This latter property, in addition to the fact that the ^{3}MC level is expected to lie at roughly the same energy within the heteroleptic and homoleptic complexes,[21] further contributes to the increase in the activation barrier between the emitting state and the nonradiative ^{3}MC (d–d) level. Based on these findings, even though the temperature dependence of the k_{nr} rate constants was not further studied, it seems reasonable to state that the energy-gap law (i.e., $E[^3MLCT]$ vs k_{nr}) does not adequately account for the observed behavior. It seems most likely that the main deactivation pathway proceeds via the thermally populated metal-centered (^{3}MC) level, as previously shown by Maestri et al. for a similar system.[21] The larger the (^{3}MLCT-^{3}MC) energy gap, the more difficult it becomes to populate the ^{3}MC level and consequently the luminescence lifetime becomes longer. This statement is further confirmed when one considers that 1) strong perturbation of the chromophore with respect to the reference P0/Ru is also detected at 77 K in a frozen matrix, in which no solvent-assisted process may take place, and 2) the triplet excited state of P0/Ru within P0 A/Ru is not sufficiently reducing (Tables 4 and 2) to transfer an electron intramolecularly to the acceptor moiety (oxidative quenching of *P0/Ru).

The overall set of data is thus indicative of a behavior that is consistent with an intramolecular, inductive, and through-bond mediated electronic effect, in accordance with our previous conclusions. The electronic effect of the acceptor substituents on the ruthenium(II) bis-terpyridyl chromophore lowers the efficiency of the ^{3}MC deactivation pathway such that nanosecond rather than the usual picosecond timescale lifetimes are observed for the phosphorescence of the P0/Ru-based luminophores at room temperature.[26] It is noteworthy that, among such *mononuclear* chromophores, there have been only very few examples of room-temperature luminescent tpy-based ruthenium complexes.[6, 21, 26a] Due to their key role within the framework of research devoted, for instance, to the mimicry (or modeling) of the photosynthetic processes and to molecular electronic devices,[5, 6] much effort has been directed towards improving the photophysical properties of these poorly efficient Ru/tpy-based photosensitizers. At least three different strategies have been reported to date. The first involves modifying the direct peripheral surroundings of the chromophoric core by attaching at the 4′-position of the tpy either a *specific* strongly electron-withdrawing substituent, namely -SO_2Me,[21, 27] or an organic fragment capable of enhancing the electronic delocalization over the tpy moiety, such as a bridging ethynyl group.[28] The second approach involves long-range monitoring that is achieved through a remote site appended to the chromophore such as an ethynylated pyrene moiety[29] or a potentially modifiable group, as in the case of a protonatable free tpy moiety.[30] The remote site may also be another complex[31] with a 2,5-thiophenediyl unit as a possible bridging spacer.[32] In the latter case, one would then be dealing with *di-* and *polynuclear* species, which are beyond the scope of the present discussion. The third strategy involves tuning of the luminescence properties by modifying the very nature of the inorganic chromophore itself. This can be achieved by using cyclometalating ligands[33] and, where necessary, by making supplementary structural changes within the coordination polyhedron by deliberately introducing steric hindrance,[34] or by using ancillary ligands such as CN^-, thereby generating a photosensitizer of the $[(tpy)Ru(CN)_3]^-$ type[35] that displays solvent-dependent luminescent properties.

The aforementioned strategies are nevertheless still somewhat restrictive as 1) an electron-withdrawing substituent such as SO_2Me is also an end-group that cannot be subsequently functionalized or modulated, 2) the rod-like ethynyl backbone is a connector that is not readily amenable to fine adjustment of the properties, and 3) the solvent is a parameter of little scope as inorganic luminophores are unfortunately rarely soluble in the whole range of common solvents. These drawbacks are overcome with the $R^1{}_2R^2TP^+$ group described herein, which is a polyvalent building block that may be used both as a terminal group with adjustable electronic properties and as an electroactive spacer, connector, or bridging element. Furthermore, the related ligand allows the integrity of the ruthenium(II) bis-terpyridyl chromophore to be preserved, as well as its appealing main topological features.

Intramolecular PET in the P1 family: Although the photophysical behavior at low temperature of the overall series of P1-based polyad systems appeared to be governed by the energy-gap law, comparison with room-temperature behavior may be very informative regarding the occurrence of hypothetical PET. Indeed, through-bond mediated electronic phenomena, such as inductive and mesomeric substituent effects, are persistent (to some extent) in a frozen rigid matrix, whereas some dynamic processes that are allowed in fluid media, such as solvent-assisted ET, are precluded.

On going from a fluid medium to a viscous glass, a blue shift in emission is observed. It originates from the higher energy required for the reorganization of the solvent molecules that accompanies the electronic redistribution over the polyad systems when excited in their charge-transfer states. Thus, when comparing the behavior at the two different temperatures, it is worthwhile referring to the corresponding model photosensitizer at the same temperature. The following observations should be emphasized:

1) Luminophores P1 bearing at least one dimethylamino electron-donating group, namely DP1, D_2P1 (and DP1 A), exhibit noticeable perturbations of their photophysical properties with respect to those of the isolated P1, at both 293 and 77 K. These perturbations, where measurable, consist of red-shifted emission wavelengths, smaller luminescence quantum yields, and generally shorter phosphorescence lifetimes. Such expected alterations of the photophysical features of P1 are clearly consistent with the previously established strong intercomponent electronic couplings. Note, however, that the existence of substituent effects does not rule out a priori the occurrence of ET phenomena.
2) In contrast, perturbations of the emission properties of the P1 photoactive site observed at room temperature for compounds based on P1 and A components only, almost completely vanish at 77 K. This difference in behavior as a function of temperature is particularly salient for the acceptor dyads, and especially for P1 A/Os. Moreover, at room temperature, the emission quantum yield of this latter dyad is only 50% of that of P1/Os. P1 A/Os also exhibits an approximately 30% shorter emission lifetime, whereas the strongly coupled donor group bearing DP1/Os and D_2P1/Os species, which emit at about the same energy or lower, display a small decrease in their luminescence quantum yields of the order of 20 to 25% and emission lifetimes shortened by only about 15%. These findings, together with the previously collected information concerning the weak electronic coupling between P1 and A, lead us to the statement that electronic substituent effects originating from the H_3TP^+ acceptor group cannot account for the observed quenching of the luminescence of P1 within P1 A/Os. The oxidative quenching of this luminescence resulting from an intramolecular PET process may therefore be proposed to account for the reported photophysical behavior of P1 A/Os. It is worth noting that, as is the case for the electronic[9] and electrochemical properties, the effect of the covalent attachment of H_3TP^+ to P1 upon the photophysical properties of the photosensitizer is similar to that reported when a strong electron acceptor, such as MV^{2+},[6a,c, 17, 24, 36] is connected to P1 by an insulating methylene spacer. However, a very weak substituent effect is likely to be operative for the P1/A ruthenium series, as evidenced by the small but significant red shifts of the emission wavelengths together with the slightly longer phosphorescence lifetimes (with respect to the parent P1/Ru) that are measured at low temperature (Table 5).
3) For the DP1 A triads, the matter of the occurrence of intramolecular PET is difficult to resolve at this stage of the discussion because of the electronic perturbation of the photophysical properties of P1 caused by the strongly coupled D subunit. Thermodynamic considerations are therefore required in order to help in the discrimination between the various possible hypotheses.

Calculated excited-state redox potentials of *P1, together with some radiative and nonradiative rate constants, are collected in Table 6.

Table 6. Excited-state properties of P1-based compounds.[a]

	Ru-based		Os-based			
	E(III/II*) [V]	E(II*/I) [V]	E(III/II*) [V]	E(II*/I) [V]	k_r [s^{-1}]	k_{nr} [s^{-1}]
P1	−0.73	+0.73	−0.82	+0.52	8.1×10^4	4.0×10^6
P1 A	−0.69	+0.71	−0.79	+0.51	6.1×10^4	5.9×10^6
P1 A_2	−0.67	+0.66	−0.76	+0.47	6.8×10^4	4.4×10^6
DP1	−0.64[b]	+0.69	−0.88	+0.48	7.2×10^4	4.8×10^6
D_2P1	−0.54[b]	+0.62	−0.87	+0.40	7.6×10^4	4.6×10^6
DP1 A	−0.64	+0.69	−0.81	+0.41	4.2×10^4	1.8×10^7

[a] See text for the determination of excited-state redox potentials; k_r and k_{nr} rate constants at room temperature. [b] Due to perturbations in the metal-centered oxidation process, which affect the determination of the oxidation potential $M^{III/II}$ of DP1/Ru and D_2P1/Ru (see text and Table 2), the corresponding excited-state redox potentials may be considered only as rough estimates.

0947-6539/02/0814-3172 $ 20.00+.50/0 *Chem. Eur. J.* **2002**, *8*, No. 14

Firstly, one may note that the excited-state redox potentials of *P1 within *P1A (and to some extent within *P1A_2), especially in the case of Os^{II} complexes, are almost the same as that of the isolated model *P1, both for oxidation and reduction. Interestingly, in the case of D*P1 A/Os, the value of E(III/II*) is also very close to that found for the native photosensitizer. This behavior is indeed reminiscent of the very weak electronic interaction between P1 and A previously addressed.

Secondly, comparison of the excited-state redox potentials of *P1 with the electrochemical data, more precisely with the first oxidation potentials of D and the first reduction potentials of A determined within the related polyad systems (Table 2), allows us to state that for monoelectronic processes:

1) all reductive quenching reactions of *P1 by D ($D-{}^*P1 \rightarrow D^+-P1^-$) are endoergonic by at least +0.2 eV, so that they would not be expected to occur;
2) all oxidative quenching reactions of *P1 by A (${}^*P1-A \rightarrow P1^+-A^-$) are also energetically disfavored by at least +0.2 eV, with the notable exceptions of the P1 A/Os and DP1 A/Os species, for which the intramolecular ET was estimated to be only slightly endoergonic with an energy difference of +0.12 eV, as well as P1 A_2/Os ($\Delta G^\circ = +0.16$ eV). Taking into account the fact that the calculated values of E(III/II*) and E(II/I*) are only rough estimates (due to the theoretical approximations made and the various experimental errors that affect the data on which they are based),[18–20, 37] one may conclude that PET phenomena with the associated formation of CS states ($P1^+-A^-$) can be reasonably postulated.

To further confirm that ET processes are indeed possible within the selected supramolecular systems, a bimolecular quenching experiment [Eq. (6)] was carried out with *P1/Os and the *N*-phenyl-2,4,6-triphenylpyridinium (p-TPH_3^+) model compounds.[8]

$$^*[Os(tterpy)_2]^{2+} + \text{p-}TPH_3^+ \rightarrow [Os(tterpy)_2]^{3+} + \text{p-}TPH_3^0 \quad (6)$$

Beyond the demonstration that an ET process could take place between *P1/Os and A, it was also found that the experimentally determined value for the rate constant ($k_Q = 6 \times 10^7\,M^{-1}s^{-1}$) of this reaction [Eq. (6)] could not account for the more efficient quenching process observed within the dyads and triad. The effective contribution of an *inter*molecular ET to the quenching mechanism observed for the polyads was thus negligible. Moreover, in view of the electronic and photophysical properties of the organic colorless D and A electroactive fragments (UV-absorbing) compared to those of *P1/Os (NIR/Vis-emitting ^{3}MLCT state), the above-reported quenching effect could not originate from an energy transfer.

The overall picture drawn from the photophysical study of P1-based polyad systems is that photoinduced electron-transfer processes (and the formation of charge-separated states) are expected to occur within P1 A/Os and DP1 A/Os supramolecular species, and to some extent within the P1 A_2/Os compound as well. To obtain direct evidence of such phenomena, transient absorption spectroscopy experiments were performed with the aim of detecting the formation of the reduced acceptor unit in the excited state. These investigations were carried out on P1 A/Os instead of DP1 A/Os, firstly because it is the less complicated case, and secondly because of the weaker differential optical densities observed for the triad.

Together with the findings from the spectroelectrochemical study, a comparative analysis of transient absorption difference spectra of P1/Os and P1 A/Os recorded under the same experimental conditions appeared to be fruitful. Indeed, the pronounced and reproducible modification of the features in the bleaching region of the ^{1}MLCT band for P1 A/Os is consistent with the concomitant formation of a broad band in the same region, at about 510 nm, which was ascribed to the absorbing reduced H_3TP^0 species ($[A]^-$). The formation of $[A]^-$ is further supported by the positive absorption maximum detected at 360 nm for P1 A/Os (see Table 3), which is not present in the difference spectrum of P1/Os 20 ns after the laser excitation (Figure 12). The capture of the photoexcited electron by the acceptor moiety is also revealed by the noticeable weakening of features corresponding to the chromophoric reduced ptpy ligands, located at around 390 and 600 nm. When quenched, the metal-to-ptpy charge-transfer state, that is the transient localization of the promoted electron on the chromophoric terpyridyl ligands, is very short-lived. In other words, the intercomponent ET process (to the acceptor subunit) is rapid. However, and as expected, the CS state is short-lived as it is no longer detected 280 ns after the laser pulse excitation. Due to 1) the intermingled contributions to transient absorption difference spectra, in particular that of the bleaching at 490 nm related to P1/Os with the increasing absorption of $[A]^-$ at about 510 nm, and 2) the time resolution of our laser setup (10 ns), the rate constant for the formation of the $P1^+-A^-$ CS state could not be accurately determined. Once formed, this CS state decays over 168 ns. For the triad DP1 A/Os, the electron-transfer rate constant leading to the initial CS state $D-P1^+-A^-$ could be estimated from Equation (7), in which $\tau_{(DP1\,A/Os)}$ is the luminescence lifetime of the triad and $\tau_{(DP1/Os)}$ is the corresponding lifetime of the DP1/Os model compounds:

$$k_{ET} = 1/\tau_{(DP1\,A/Os)} - 1/\tau_{(DP1/Os)} \quad (7)$$

It was found that $k_{ET} = 1.27 \times 10^7\,s^{-1}$. Taking into account the fact that the subsequent net transfer of one electron from the donor D (competing with the charge recombination process) to give D^+-P1-A^- is, as expected, unlikely on the basis of thermodynamic considerations (Tables 6 and 2),[9] the shortened lifetime of 57 ns (Table 5) may be rationalized in terms of an enhanced electron-releasing *inductive effect* from D when it is connected to the oxidized and positively charged $[{}^*P1]^+$ (in the excited state) as compared to P1 in the ground state.

In summary, it has been demonstrated that, under certain conditions, P1-photosensitized supramolecular species based on the new triphenylpyridinium-derivatized ptpy ligands do undergo PET processes, leading to charge-separated states.

Conclusion

Although the chemical variability (R^1, R^2) of the novel $R^1{}_2R^2TP^+$-(p)$_n$tpy family of ligands[8, 9] has not yet been exploited,[38] electrochemical studies have shown that the redox properties of the electron-acceptor fragment can be tuned, as expected, through changing its peripheral substituents (in the present case by changing the *N*-aryl group of the pyridinium ring). In its native form ($R^1 = R^2 = H$), the H_3TP^+ moiety is a weak acceptor that can be reduced in two one-electron steps in a narrow potential range, which may be adjusted to give a single two-electron step of potential interest for multi-electron purposes such as catalysis.

The P0- and P1-based systems show different photophysical behavior. Interestingly, when H_3TP^+ is directly connected to the nonluminescent $Ru(tpy)_2{}^{2+}$ chromophore (P0/Ru), the photophysical properties of this complex are modified in such a manner that the photosensitizer becomes a good luminophore at room temperature. This result is obtained without any loss of the precious structural features of the native chromophore. Furthermore, owing to chemical versatility of the novel $R^1{}_2R^2TP^+$-tpy ligand, the corresponding complex can be used as an efficient photosensitizing building block with adjustable properties, both in a terminal position and in an internal position within polynuclear rigid rodlike supermolecules ($R^1{}_2R^2TP^+$-tpy is then transformed into a connecting or bridging ligand).

When a phenyl spacer is present (P1 family), it has been shown that, under particular conditions (Os series), a CS state can be reached as a result of PET processes between P and A. However, the weakness of H_3TP^+ as an electron acceptor prevents the CS states from being easily produced within all the investigated polyad systems. On the basis of the evident tunability of $R^1{}_2R^2TP^+$, however, it should be possible[38] to make A more efficient for generating long-range and long-lived CS states within redox cascades or branched superstructures.

In conclusion, these results clearly show the possibility of designing novel photosensitized molecular and supramolecular inorganic systems based on the triarylpyridinium unit, for potential applications in solar energy conversion and molecular electronics or photonics (such as nonlinear optic properties[39]).

Experimental Section

Materials: All compounds were synthesized as described elsewhere.[9]

Electrochemical and spectroelectrochemical measurements: The electrochemical experiments were carried out with a conventional three-electrode cell (solution volume 15 mL) and a PC-controlled potentiostat/galvanostat (Princeton Applied Research model 263 A). The working electrode, which was mounted in Teflon, was a platinum disk from Radiometer – Tacussel with an exposed geometrical area of 0.032 cm^2. Hydrodynamic voltammetry experiments were conducted by rotating the disk electrode at various rates, ranging from 400 to 3600 rpm (Controvit device from Radiometer – Tacussel, France). The electrode was polished before each experiment with 3 μm and 0.3 μm alumina pastes followed by extensive rinsing with ultrapure Milli-Q water. Platinum wire was used as the counter electrode, while a saturated calomel electrode (SCE) served as the reference electrode. Electrolytic solutions, acetonitrile containing 0.1M tetrabutylammonium tetrafluoroborate ($TBABF_4$, Aldrich, 99 % +) as supporting electrolyte, were routinely deoxygenated by argon bubbling. All potentials are quoted with respect to the SCE.

Cyclic voltammetric data were used to estimate formal potentials $E_{1/2}$ as $(E_{pa} + E_{pc})/2$, in which E_{pa} and E_{pc} are the anodic and cathodic peak potentials, respectively, relating to the redox process under consideration. In some cases, $E_{1/2}$ was evaluated directly from the hydrodynamic voltammograms as being the half-wave potential value. Standard rate constants k° for electron-transfer reactions under kinetic-diffusion-controlled conditions were estimated from the cyclic voltammogram peak separations using the established method of Nicholson.[40] For this purpose, diffusion coefficients of the relevant species in solution were calculated from hydrodynamic voltammetry data by using Levich's equation,[40a] and the number of electrons involved in the redox process was determined by comparison with reference components. It was surmised that ohmic drop was minimal under the experimental conditions used, and did not affect the potential peak separation and k° calculations.

In situ spectroelectrochemical measurements were carried out in a home-made cell consisting of a standard UV/Vis cuvette (pathlength 1 cm; total solution volume 5.5 mL), of which the top had been opened out to allow the easy introduction of the working, reference, and counter electrodes. The working electrode was a platinum grid of geometrical area 3 cm^2, which was flattened against one of the walls of the cuvette opposite to the light beam pathway. Platinum wire was used as the counter electrode, and home-made AgCl-coated Ag wire was used as the reference electrode. The potential difference between this reference electrode and SCE amounted to 30 mV, and this value was checked daily, before and after use. Electrolytic solutions were routinely deoxygenated with argon and kept under inert atmosphere during the experiments. UV/Vis data were recorded with a Shimadzu UV-160 A spectrophotometer.

Photophysical properties: The uncorrected emission spectra were recorded on a Jobin Yvon Spex Fluorolog FL 111 spectrofluorimeter. Emission quantum yields for argon-degassed solutions of the complexes of the P0/Ru series in acetonitrile were determined relative to a solution of $[Ru(bpy)_3]^{2+}$ in acetonitrile ($\Phi_{em} = 6.2 \times 10^{-2}$) as a reference.[18] For the P1/Os series, the reference was $[Os(bpy)_3]^{2+}$ in acetonitrile ($\Phi_{em} = 5 \times 10^{-3}$).[41] Excitation spectra were corrected according to the lamp spectrum. The optical density of each solution was adjusted to 0.1 at the excitation wavelength.

Transient absorption spectra and excited-state lifetimes were determined by laser flash spectroscopy. The nanosecond setup has been described in detail elsewhere.[36] Briefly, an excimer laser (Lambda Physik EMG 100, 308 nm pulses of duration 10 ns and energy 150 mJ) was used as the excitation source. The detection system consisted of a xenon flash lamp, a Jobin Yvon H25 monochromator, a Hamamatsu R955 photomultiplier, and a Le Croy 9362 digital oscilloscope. The laser intensity was attenuated to avoid biphotonic effects. The analysis was carried out within the first millimeter of the sample excited by the laser pulse, with quartz cells of 1 cm pathlength (room temperature experiments). The optical density of the samples was adjusted to 0.8 at the excitation wavelength of the laser ($\lambda_{exc} =$ 308 nm). All photophysical properties were measured in acetonitrile (Aldrich, 99.5 %, spectrophotometric grade) at room temperature and in butyronitrile (Aldrich, 99 % +) at 77 K. For the low-temperature measurements, cylindrical quartz cells were used, and the solutions were cooled in a quartz Dewar containing liquid nitrogen. Solutions were deaerated either by bubbling with argon (room temperature experiments) or by vacuum degassing through successive freeze-pump-thaw cycles (low temperature experiments)

Room-temperature, picosecond experiments on compounds of the P1/Ru series were carried out with a mode-locked, frequency-doubled Nd:YAG laser (532 nm pulses of duration 25 ps and energy 12 mJ).[42] Triplet lifetimes were measured by transient absorption spectroscopy, following the recovery of ground state at 490 nm (experimental uncertainty ± 20 ps). Solutions of the complexes in acetonitrile (at 293 K) were deoxygenated prior to laser flash photolysis.

Acknowledgements

We are particularly grateful to Prof. Anthony Harriman for carrying out the room-temperature picosecond photophysical experiments on the P1-based

  0947-6539/02/0814-3174 $ 20.00+.50/0

ruthenium compounds. Prof. Jean-Pierre Launay is warmly acknowledged for fruitful discussions. P.L. is indebted to Dr. Valérie Marvaud for her indestructible support.

[1] a) J.-M. Lehn, *Supramolecular Chemistry*, VCH, Weinheim, **1995**; b) J.-M. Lehn, *Angew. Chem.* **1988**, *100*, 91–116; *Angew. Chem. Int. Ed. Engl*. **1988**, *27*, 89–112.

[2] a) See, for instance, the special issue on Molecular Machines, *Acc. Chem. Res.* **2001**, *34*, 409–522; b) For a extensive survey, see, for instance: *Comprehensive Supramolecular Chemistry* (Eds.: J. L. Atwood, J. E. D. Davies, D. D. McNicol, F. Vögtle), Pergamon, Oxford, **1996**.

[3] a) H. Dürr, S. Bossmann, *Acc. Chem. Res.* **2001**, *34*, 905–917, and references therein; b) D. Gust, T. A. Moore, A. L. Moore, *Acc. Chem. Res.* **2001**, *34*, 40–48, and references therein.

[4] a) J.-M. Lehn, *Angew. Chem.* **1990**, *102*, 1347–1362; *Angew. Chem. Int. Ed. Engl*. **1990**, *29*, 1304–1319; b) "*Supramolecular Photochemistry*": V. Balzani, L. Moggi, F. Scandola, *NATO ASI Ser. Ser. C***1987**, *214*, 1–28.

[5] a) V. Balzani, A. Juris, M. Venturi, S. Campagna, S. Serroni, *Chem. Rev.* **1996**, *96*, 759–833; b) V. Balzani, F. Scandola, *Supramolecular Photochemistry*, Horwood, Chichester, **1991**.

[6] a) J.-P. Collin, P. Gaviña, V. Heitz, J.-P. Sauvage, *Eur. J. Inorg. Chem*. **1998**, 1–14, and references therein; b) F. Barigelletti, L. Flamigni, J.-P. Collin, J.-P. Sauvage, *Chem. Commun*. **1997**, 333–338; c) J.-P. Sauvage, J.-P. Collin, J.-C. Chambron, S. Guillerez, C. Coudret, V. Balzani, F. Barigelletti, L. De Cola, L. Flamigni, *Chem. Rev.* **1994**, *94*, 993–1019, and references therein.

[7] A. Nakano, A. Osuka, T. Yamazaki, Y. Nishimura, S. Akimoto, I. Yamazaki, A. Itaya, M. Murakami, H. Miyasaka, *Chem. Eur. J.* **2001**, *7*, 3134–3151.

[8] P. Lainé, E. Amouyal, *Chem. Commun*. **1999**, 935–936.

[9] P. Lainé, F. Bedioui, P. Ochsenbein, V. Marvaud, M. Bonin, E. Amouyal, *J. Am. Chem. Soc*. **2002**, *124*, 1364–1377.

[10] C. Reichardt, *Chem. Rev.* **1994**, *94*, 2319–2358, and references therein.

[11] M. Martiny, E. Steckhan, T. Esch, *Chem. Ber.* **1993**, *126*, 1671–1682.

[12] S. Tripathi, M. Simalty, J. Pouliquen, J. Kossanyi, *Bull. Soc. Chim. Fr*. **1986**, *4*, 600–612.

[13] F. Würthner, A. Sautter, C. Thalacker, *Angew. Chem.* **2000**, *112*, 1298–1301; *Angew. Chem. Int. Ed.* **2000**, *39*, 1243–1245.

[14] E. T. Seo, R. F. Nelson, J. M. Fritsch, L. S. Marcoux, D. W. Leedy, R. N. Adams, *J. Am. Chem. Soc*. **1966**, *88*, 3498–3503.

[15] The determination of the exact nature of the putative electrocatalytic process is beyond the scope of this paper and will be discussed elsewhere.

[16] One may consequently determine the associated comproportionation equilibrium constant K_c (with $Os^{III} = P1/Os^{+}$), [Eq. (8a)], which accounts for the relative abundance of homovalent and mixed-valent species in solution for the reaction according to Equation (8b), by using the relationship shown as Equation (8c) (with $T = 293$ K, $n = 1$, and $\Delta E = 0.155$ V) [see D. E. Richardson, H. Taube, *Inorg. Chem*. **1981**, *20*, 1278–1285].

$$K_c = [D^{+} - Os^{III} - D]^2/[D^{+} - Os^{III} - D^{+}] \times [D - Os^{III} - D] \quad (8a)$$

$$[D_2P1/Os]^{3+} + [D_2P1/Os]^{5+} \rightleftharpoons 2[D_2P1/Os]^{4+} \quad (8b)$$

$$RT\ln K_c = nF\Delta E \quad (8c)$$

A rather large value of K_c (≈ 464) is obtained for an estimated formal inter-site distance of 20 Å. Actually, this value becomes more reasonable if one takes into account the postulated participation of the Os^{III} cation, which has rather diffuse d orbitals, the electrostatic interaction then being mediated over an actual distance of only about 10 Å. Indeed, a K_c value of 600 has been found for a homodinuclear complex of Ru^{II} bridged by the 3,3′,5,5′-tetrapyridylbiphenyl biscyclometalating ligand, which has a length of 11 Å [see M. Beley, J.-P. Collin, R. Louis, B. Metz, J.-P. Sauvage, *J. Am. Chem. Soc*. **1991**, *113*, 8521–8522].

[17] J.-P. Collin, S. Guillerez, J.-P. Sauvage, F. Barigelletti, L. De Cola, L. Flamigni, V. Balzani, *Inorg. Chem.* **1992**, *31*, 4112–4117.

[18] a) J. V. Caspar, T. J. Meyer, *Inorg. Chem.* **1983**, *22*, 2444–2453; b) J. V. Caspar, T. J. Meyer, *J. Am. Chem. Soc.* **1983**, *105*, 5583–5590.

[19] E. M. Kober, J. L. Marshall, W. J. Dressick, B. P. Sullivan, J. V. Caspar, T. J. Meyer, *Inorg. Chem.* **1985**, *24*, 2755–2763.

[20] a) T. J. Meyer, *Pure Appl. Chem.* **1986**, *58*, 1193–1206; b) A. Juris, V. Balzani, F. Barigelletti, P. Belser, A. Von Zelewsky, *Coord. Chem. Rev*. **1988**, *84*, 85–277.

[21] M. Maestri, N. Armaroli, V. Balzani, E. C. Constable, A. M. W. Cargill Thompson, *Inorg. Chem*. **1995**, *34*, 2759–2767.

[22] V. Grosshenny, A. Harriman, R. Ziessel, *Angew. Chem.* **1995**, *107*, 1211–1214; *Angew. Chem. Int. Ed. Engl.* **1995**, *34*, 1100–1102.

[23] One may note that the points corresponding to the Ru series are somewhat scattered within a narrow energy range of about 0.1 eV. It is thus difficult to establish a priori that the related emission lifetimes follow the energy-gap law. However, such scattering of the values was also observed by Maestri et al.[21] for another series of Ru tpy complexes with electron-accepting and -donating substituents, and this was attributed to some specific although not yet clearly identified influences of the substituents present. On the other hand, Caspar and Meyer[18, 19] have shown that the slopes determined from linear relationships for series of bipyridyl complexes of Ru and Os are identical within experimental error. Taking into account this result, one may analyze P1/Ru- and P1/Os-based compounds collectively. Figure 11 shows that a linear correlation can indeed be found for the present ensemble of Ru and Os bis-terpyridyl complexes, having a slope of -6.29 and an intercept of 23.6, similar to the values reported in the literature.[18, 19]

[24] J.-P. Collin, S. Guillerez, J.-P. Sauvage, F. Barigelletti, L. De Cola, L. Flamigni, V. Balzani, *Inorg. Chem.* **1991**, *30*, 4230–4238.

[25] Interestingly, beyond these cumulative properties, it is noteworthy that the electron added to the acceptor fragment is also partially delocalized over the photosensitizer, as evidenced by the chromophoric signature of $[P1/Os]^{-}$. Consequently, the photoinduced excited-state charge separation $*(P1^{+} - A^{-})$ can be expected to be short-lived, a fortiori, as it involves the reduced acceptor $[A]^{-}$ and the oxidized photosensitizer $[P1/Os]^{+}$ instead of the native P1/Os.

[26] a) M. Beley, J.-P. Collin, J.-P. Sauvage, H. Sugihara, F. Heisel, A. Miehé, *J. Chem. Soc. Dalton Trans.* **1991**, 3157–3159; b) E. Amouyal, M. Mouallem-Bahout, G. Calzaferri, *J. Phys. Chem.* **1991**, *95*, 7641–7649; c) J. R. Winkler, T. L. Netzel, C. Creutz, N. Sutin, *J. Am. Chem. Soc.* **1987**, *109*, 2381–2392; d) J. R. Kirchhoff, D. R. McMillin, P. A. Marnot, J.-P. Sauvage, *J. Am. Chem. Soc.* **1985**, *107*, 1138–1141; e) M. L. Stone, G. A. Crosby, *Chem. Phys. Lett*. **1981**, *79*, 169–173.

[27] E. C. Constable, A. M. W. Cargill Thompson, N. Armaroli, V. Balzani, M. Maestri, *Polyhedron* **1992**, *20*, 2707–2709.

[28] A. C. Benniston, V. Grosshenny, A. Harriman, R. Ziessel, *Angew. Chem.* **1994**, *106*, 1956–1958; *Angew. Chem. Int. Ed. Engl.* **1994**, *33*, 1884–1885.

[29] A. Harriman, M. Hissler, A. Khatyr, R. Ziessel, *Chem. Commun*. **1999**, 735–736.

[30] F. Barigelletti, L. Flamigni, M. Guardigli, J.-P. Sauvage, J.-P. Collin, A. Sour, *Chem. Commun*. **1996**, 1329–1330.

[31] L. Hammarström, F. Barigelletti, L. Flamigni, M. T. Indelli, N. Armaroli, G. Calogero, M. Guardigli, A. Sour, J.-P. Collin, J.-P. Sauvage, *J. Phys. Chem. A* **1997**, *101*, 9061–9069.

[32] E. C. Constable, C. E. Housecroft, E. R. Schofield, S. Encinas, N. Armaroli, F. Barigelletti, L. Flamigni, E. Figgemeier, J. G. Vos, *Chem. Commun*. **1999**, 869–870.

[33] M. Beley, S. Chodorowski, J.-P. Collin, J.-P. Sauvage, L. Flamigni, F. Barigelletti, *Inorg. Chem.* **1994**, *33*, 2543–2547.

[34] J.-P. Collin, R. Kayhanian, J.-P. Sauvage, G. Calogero, F. Barigelletti, A. De Cian, J. Fischer, *Chem. Commun*. **1997**, 775–776.

[35] M. T. Indelli, C. A. Bignozzi, F. Scandola, J.-P. Collin, *Inorg. Chem*. **1998**, *37*, 6084–6089.

[36] E. Amouyal, M. Mouallem-Bahout, *J. Chem. Soc. Dalton Trans.* **1992**, 509–513.

[37] C. Berg-Brennan, P. Subramanian, M. Absi, C. Stern, J. T. Hupp, *Inorg. Chem*. **1996**, *35*, 3719 – 3722.
[38] Work in progress.
[39] M. Konstantaki, E. Koudoumas, S. Couris, P. Lainé, E. Amouyal, S. Leach, *J. Phys. Chem. B* **2001**, *105*, 10797 – 10804.
[40] a) A. J. Bard, L. R. Faulkner, *Electrochemical Methods: Fundamentals and Applications*, 2nd ed., Wiley, New York, **2001**; b) R. S. Nicholson, *Anal. Chem.* **1965**, *37*, 1351 – 1355.
[41] E. M. Kober, J. V. Caspar, R. S. Lumpkin, T. J. Meyer, *J. Phys. Chem.* **1986**, *90*, 3722 – 3734.
[42] A. Harriman, M. Hissler, P. Jost, G. Wipff, R. Ziessel, *J. Am. Chem. Soc.* **1999**, *121*, 14 – 27.

Received: December 21, 2001 [F3757]

  0947-6539/02/0814-3176 $ 20.00+.50/0